

# Total external reflection from metamaterials with ultralow refractive index

Brian T. Schwartz and Rafael Piestun

*Department of Electrical and Computer Engineering, University of Colorado at Boulder,  
Boulder, Colorado 80309-0425*

Received November 14, 2002; revised manuscript received July 29, 2003; accepted August 5, 2003

Metamaterials composed of metal-dielectric nanostructures are engineered to have an effective refractive index less than unity at optical wavelengths. The effect of total external reflection is demonstrated when light from vacuum is incident onto these materials at an angle exceeding the critical angle defined by Snell's law. Novel approaches are discussed to derive the effective index of refraction from the reflection and refraction properties of finite slabs. The effect of losses and dispersion are analyzed in the visible range of frequencies by consideration of the measured properties of silver. The differences among ultralow refractive-index metamaterials, photonic bandgap materials, and metals are discussed. Remarkably, a bandgap is not required to obtain total external reflection. © 2003 Optical Society of America

OCIS codes: 050.1970, 160.4670, 350.3950.

## 1. INTRODUCTION

There has been a growing interest in the optical properties of micro- and nanostructured materials because of their ability to control light in unconventional ways. Research on photonic crystals has been focused on engineering bandgaps for a variety of applications.<sup>1</sup> Lately several groups have reported intriguing physical properties of metamaterials presenting simultaneous negative permittivity and permeability.<sup>2-6</sup> However, the implementation of these so-called negative-index materials in the optical regime is still a challenging task.

Nevertheless, in many photonic structures composed of two or more dielectrics, such as waveguides and photonic bandgap structures, the absolute value of the index contrast is more important than the sign of the indices. Therefore increasing this contrast would be extremely useful, and ultralow refractive-index materials (ULIMs) can achieve this goal.<sup>7</sup>

Current nanofabrication techniques can generate feature sizes much smaller than visible wavelengths, thus allowing the fabrication of these metamaterials in the optical regime. However, in this regime the limitations of nanofabrication and the scaling of physical properties of metals and dielectrics require special attention.

In this paper we propose the use of metamaterials with the real part of the effective index less than unity ( $0 \leq \text{Re}\{n_{\text{eff}}\} \leq 1$ ) as a building block for photonic applications.<sup>7</sup> First, we discuss basic phenomena and the feasibility of metal-dielectric structures with  $0 \leq \text{Re}\{n_{\text{eff}}\} \leq 1$  by using approximate analytical models. We then study the refraction and reflection properties of finite slabs of the metamaterial by using numerical models and show that total external reflection (TER) from air is possible with simple structures. Finally, we discuss the effects of losses and dispersion and compare these metamaterials with photonic bandgap materials and bulk metals.

## 2. BACKGROUND RESEARCH AND ITS RELATION TO ULTRALOW REFRACTIVE-INDEX MATERIALS

Metamaterials, an extension of the concept of artificial dielectrics, were first designed in the 1940s for microwave frequencies.<sup>8</sup> They typically consist of periodic geometric structures of a guest material embedded in a host material. Just as homogeneous dielectrics owe their optical properties to the nanometer-scale structure of its atoms, metamaterials derive their properties from the subwavelength structure of its component materials. At wavelengths much longer than the unit-cell size, the structure can be assigned parameters that describe homogeneous dielectrics, such as electric permittivity and refractive index. Over the years, the analysis of artificial composite materials has been carried out under several frameworks such as transmission-line models,<sup>8</sup> effective-medium theory,<sup>9</sup> homogenization,<sup>10</sup> and photonic crystals.<sup>1</sup>

As long as 50 years ago, it was recognized that artificial dielectrics can have an effective index of refraction below unity.<sup>11</sup> Investigations have shown its potential application in the design of antennas,<sup>8,12</sup> including a report that appeared while this paper was under review.<sup>13</sup> Recent investigations have also shown the potential of zero-permittivity materials as bandgap structures.<sup>14</sup> This is a limiting case of the ULIMs when losses are neglected ( $\epsilon_{\text{eff}} = 0$  leads to  $n_{\text{eff}} = 0$ ). Low-permittivity materials are related to what is known in electromagnetics as high-impedance surfaces.<sup>15</sup>

It should be noted, however, that these investigations do not provide a proper analysis of the behavior of ULIMs in the visible regime. At these frequencies, metal losses and dispersion become critical and cannot be neglected. In addition, features much smaller than the wavelength are hard to fabricate, and thus, in general, the long-wavelength approximation does not hold.

The goal of this paper is to analyze the reflection and

transmission properties of ULIMs at optical frequencies. In particular, we investigate for the first time, to our knowledge, the effect of TER as defined by a critical angle in Snell's law.

Total internal reflection is a very well-known optical effect and is the basis of various technologies such as index waveguides, polarizing devices, and near-field microscopes. Similarly, TER occurs when light propagating in vacuum is incident on a medium with a refractive index less than unity at an angle exceeding the critical angle defined by Snell's law. This effect is very well known for x rays incident on planar interfaces at grazing angles.<sup>16</sup> In the x-ray regime the index of refraction is expressed in the form  $n = 1 - \delta + i\beta$ , where, typically,  $\delta \approx 10^{-5}$  and  $\beta \approx 10^{-7}$ . For angles exceeding the critical angle, as defined for the lossless case, the refracted waves are inhomogeneous, the refracted angle is very close to  $\pi/2$ , and the reflectivity is very close to unity.<sup>16</sup> Here, in contrast, we describe metamaterials exhibiting TER at visible wavelengths. The real part of the refractive index is well below unity ( $0 < \delta \leq 1$ ), and the loss component is small compared with bulk metals ( $\beta \ll 1$ ).

### 3. THEORY

Effective-medium theories allow the characterization of the electromagnetic properties of composite materials when the wavelength is much larger than the unit cell in periodic composites or the scale of the particles in disordered composites. The properties depend on the host permittivity, the guest permittivity, the volume fraction, the frequency, and the morphology of the composite material. When all other variables are given, changes in the morphology allow for a wide range of values in the permittivity and permeability.<sup>9</sup>

To demonstrate the design of ULIMs, we have chosen a simple structure consisting of an array of metallic cylindrical wires embedded in air. Above the cutoff frequency of the structure, the metamaterial behaves like a homogeneous material with permittivity below unity. These metamaterials are lossy so their refractive index is, in fact, complex, the real part satisfying  $0 \leq \text{Re}\{n_{\text{eff}}\} \leq 1$ .

We used an approximate analytic model as a starting point in the design of a structure with  $0 \leq \text{Re}\{n_{\text{eff}}\} \leq 1$  at  $\lambda = 0.5 \mu\text{m}$  for light polarized parallel to the wires (and thus propagating normal to the wire axes) (Fig. 1). The

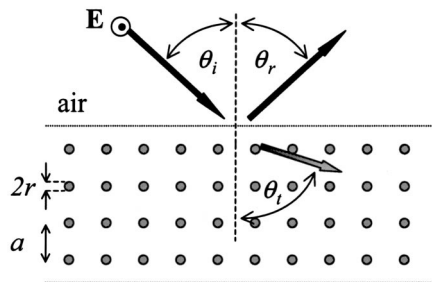


Fig. 1. Refraction and reflection at the interface of air and a two-dimensional metamaterial with ultralow effective refractive index. Light is refracted off the normal to the surface, and the refracted waves are inhomogeneous. In the specific design the metamaterial is composed of a square array of cylindrical wires, and the incident light is polarized parallel to the wires.

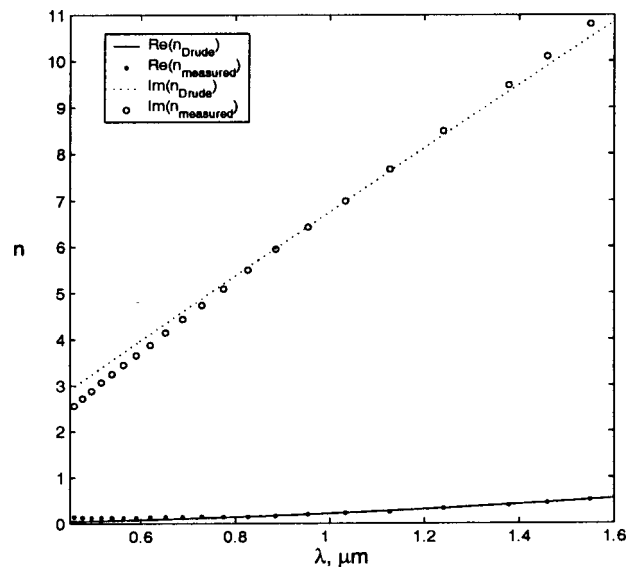


Fig. 2. Experimental values and best-fit Drude model predictions ( $\nu_p^{\text{Ag}} = 1174.8 \text{ THz}$ ,  $\gamma^{\text{Ag}} = 205.2 \text{ THz}$ ) for the refractive index of silver for wavelengths between  $0.45$  and  $1.6 \mu\text{m}$ .

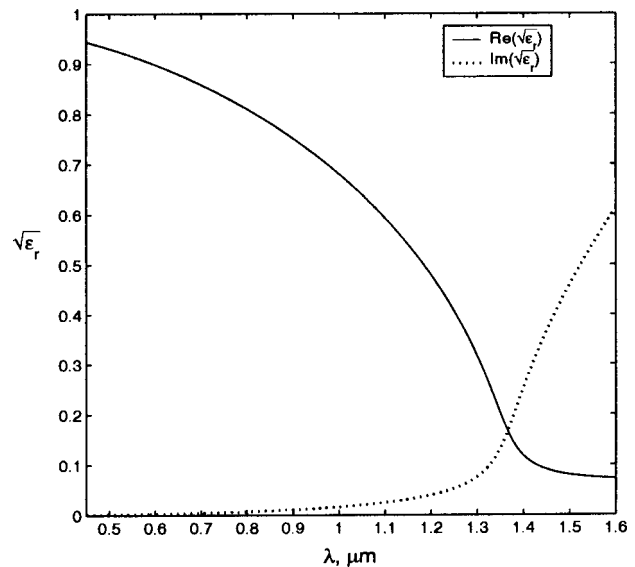


Fig. 3. Square root of the effective relative dielectric constant [Eq. (1)] of a silver-air metamaterial as a function of free-space wavelength. Wire radius,  $r = 15 \text{ nm}$ ; unit-cell size,  $a = 200 \text{ nm}$ .

model provides an effective relative dielectric constant  $\epsilon_{r\perp}(\omega)$  as a function of frequency  $\omega$  according to the expression

$$\epsilon_r = 1 - \frac{\omega_p^2}{\omega(\omega + i\gamma)}, \quad (1)$$

where  $\omega_p$  is the analog of the plasma frequency and  $\gamma$  is a damping frequency. These parameters depend on the unit-cell geometry and the conductivity of the metal  $\sigma(\omega)$  and can be calculated as  $\omega_p^2 = 2\pi c_0^2/a^2 \ln(a/r)$  and  $\gamma = \epsilon_0 a^2 \omega_p^2 / \pi r^2 \sigma$ ,<sup>17</sup> where  $a$  is the period,  $r$  is the radius, and  $c_0$  is the speed of light in vacuum; the parameters are valid for  $r \ll a$ . The expression for complex frequency-

dependent conductivity is  $\sigma = \epsilon_0(\omega_p^{\text{Ag}})^2/(\gamma^{\text{Ag}} - i\omega)$ ,<sup>18</sup> where  $\omega_p^{\text{Ag}}$  and  $\gamma^{\text{Ag}}$  are the plasma frequency and electron collision frequency of silver. We obtained these parameters by fitting the Drude model to measured refractive-index values in the frequency range of interest<sup>19</sup> (Fig. 2).

This type of model can be interpreted in terms of conventional electrodynamics and can be derived in several ways, including transmission-line models and homogenization theory.<sup>10,20–22</sup> It has also shown fair agreement with numerical and experimental results.<sup>17</sup> Although approximate, this model takes into account the effects of polarization, dispersion, losses, and geometry of the metamaterial.

Hence we first used Eq. (1) as a guide to find the geometry of a wire array with  $0 < \text{Re}\{\epsilon_{r,\perp}\} < 1$  at  $\lambda = 0.5 \mu\text{m}$ , and then we studied the optical properties by using numerical models. For silver wires of radius  $r = 15 \text{ nm}$  in a square lattice with  $a = 200 \text{ nm}$  unit cells, the effective resonance wavelength is  $\lambda_p = 0.8 \mu\text{m}$ , and the effective (relative) dielectric constant  $\epsilon_{\text{eff}}$  is between zero and 1 at slightly shorter wavelengths (Fig. 3). We considered these predictions to be approximate because the unit-cell length is just less than half the minimum operating wavelength. Note that this structure also has an effective permeability that, in general, is different from unity,<sup>8</sup> thus affecting the effective index.

#### 4. DISPERSION DIAGRAM

The calculated dispersion curves for the first few modes of the specified wire array composed of perfect conductors are shown in Fig. 4. The calculations were performed by a finite-element Maxwell's equation solver.<sup>23</sup> The difference between the left-hand ( $\Gamma - X$ ) and right-hand ( $M - \Gamma$ ) sides of the dispersion curve shows that the metamaterial is anisotropic. This anisotropy disappears in the long-wavelength limit. Figure 4 shows that the

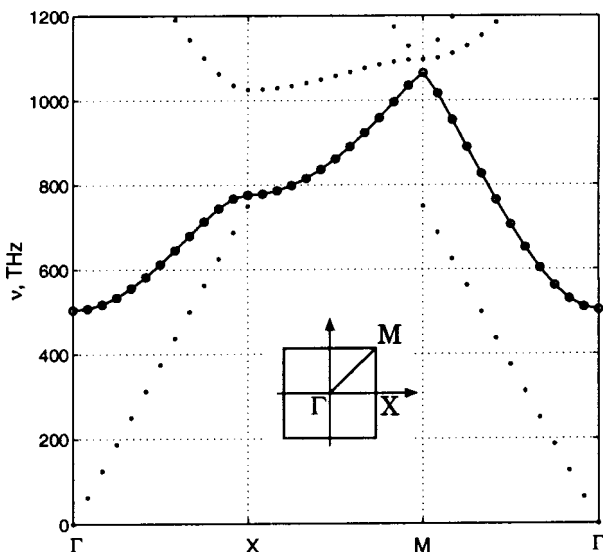


Fig. 4. Dispersion diagram of a two-dimensional square array of silver wires. The wires have radius  $r = 15 \text{ nm}$  and are spaced  $200 \text{ nm}$  apart. The two straight lines are the dispersion curves of light in free space.

lowest-frequency mode is above the light line, which suggests that the wire array has an effective refractive index  $n_{\text{eff}} = ck/\omega$  less than unity in agreement with the analytical model. For the design frequency (600 THz), there is only one propagating mode, a necessary condition to assign a well-defined refractive index to a metamaterial. Also note the absence of a bandgap in the region of interest, which differentiates the nature of the ultralow refractive index discussed here from other related effects that require a bandgap.<sup>24</sup>

An approximate effective index could be obtained from the phase velocity of the propagating mode  $v = \omega/k$  inside the infinitely periodic structure. However, such an effective index is not accurate because the model does not account for the finiteness of real structures.<sup>25,26</sup> In effect, evanescent modes at the boundaries of finite structures ensure field continuity at interfaces. Because  $a/\lambda \leq 1/2$ , these modes are more significant than in structures with smaller  $a/\lambda$  values, so neglecting this effect can lead to inaccuracies in the predicted effective index.

#### 5. REFRACTION AT A PLANAR INTERFACE AND CALCULATION OF THE EFFECTIVE INDEX

Both the analytic model and the dispersion curves provide only an approximate qualitative prediction for the refractive index. Calculating an accurate effective refractive index requires numerical techniques that account for losses and the finite character of real structures. Hence we calculated the refracted fields when a plane wave is incident normal to a planar air–metamaterial interface. The refracted waves are inhomogeneous because of the metal losses, which correspond to a complex refractive index. For the metamaterial to have an effective index less than 1, it must properly refract light. That is, light must propagate inside the metamaterial the same way it would in a transparent homogeneous material with  $\text{Re}\{n\} < 1$ , should one exist.

We used a finite-element Maxwell's equations solver<sup>27</sup> to compute the fields refracted by the metamaterial, as shown in Fig. 5. To determine the metamaterial's effective index at each wavelength, we used a minimization algorithm to find the refractive index of a homogeneous material that transmits the same electric field as the metamaterial (inhomogeneous plane wave with the same complex propagation constant). The algorithm required an initial guess for the complex refractive index, and the resulting effective index values are insensitive to these guesses to four decimal places. This method for calculating  $n_{\text{eff}}$  differs from previous methods,<sup>8,25,28</sup> which rely on the reflection coefficients and present ambiguity in the phase of the reflected wave.

Accurate modeling of metamaterials in the optical regime requires consideration of losses and materials' dispersion. In our simulations, we used interpolated values of the refractive index of silver, shown in Fig. 2.

Figure 6 shows the calculated effective index confirming that indices with the real part below unity are feasible at optical frequencies. Although the general behavior coincides with the predictions of the analytical models (Fig. 3), the numerical model predicts different effective

plasma wavelengths. This occurs in part because the accuracy of the analytical model requires  $\lambda \gg a$ . The metamaterial's fairly low loss [ $\text{Im}(n_{\text{eff}}) \ll 1$ ] is a promising property for practical purposes.

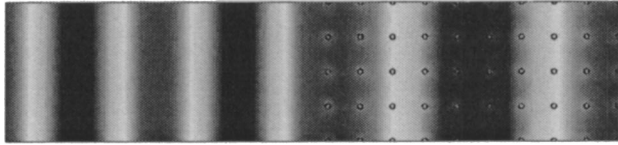


Fig. 5. Electric field magnitude (parallel to the wires) of  $\lambda_0 = 1.0 \mu\text{m}$  light normally incident on a silver-air metamaterial.

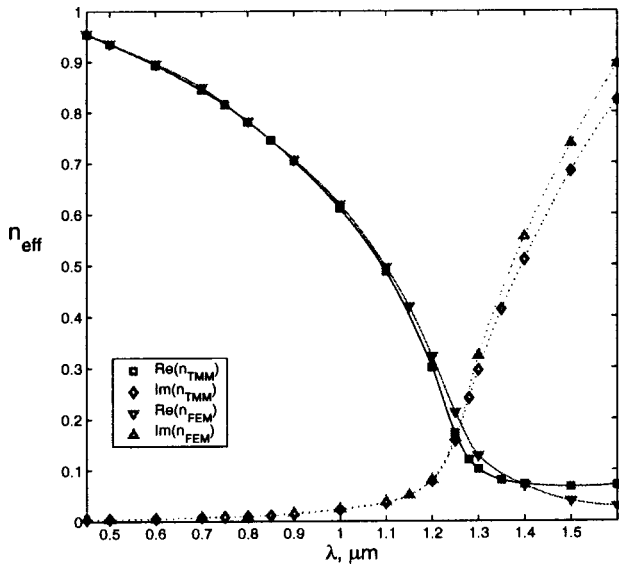


Fig. 6. Refractive index (real and imaginary parts) of the metamaterial as a function of a free-space wavelength as predicted by its normal incidence refraction (finite-elements method) and angle-dependent reflectivity (TMM). Wire radius,  $r = 15 \text{ nm}$ ; unit-cell size,  $a = 200 \text{ nm}$ .

## 6. REFLECTION AT A PLANAR INTERFACE

ULIMs have interesting reflection properties because the real part of the index is lower than the index of air. Therefore Snell's law predicts a critical angle above which total reflection occurs. We studied numerically the TER for slabs of ULIMs and used the reflectivity at all angles to calculate the effective index, which was compared with the results obtained by refraction (Section 5).

The transfer-matrix method<sup>29,30</sup> (TMM) was used to find the reflectivity  $\mathcal{R}_{\text{TE}}$  and transmissivity  $\mathcal{T}_{\text{TE}}$  of ULIM slabs of different thicknesses at  $\lambda_0 = 0.5 \mu\text{m}$ . Figures 7 and 8 show the reflection and transmission properties of slabs containing 1 to 128 periods of the array and a comparison to equivalent homogeneous slabs with the same thickness and index. The thickness of the equivalent slab was determined as the number of layers multiplied by the unit-cell width. The interface plane was chosen at a distance equal to half unit-cell width before the first wire row (Fig. 1). A  $30 \times 30$  grid was used in the TMM to properly sample the two-dimensional unit cell. We verified this by increasing the sampling to a  $60 \times 60$  grid and obtaining the same effective index as discussed below. The dielectric constant of silver was obtained from experimental data as before (Fig. 2).

The structure behaves like a lossy dielectric with a refractive index less than unity for light polarized normal to the incident plane (TE) and parallel to the wires. At small incident angles there is little reflection, whereas at larger angles the structure abruptly becomes reflective. The reflectivity of a dielectric slab with an index of  $n = 0.935 + 0.0038i$  fits the reflectivity of the wire arrays with four or more periods. The critical angle, defined here as the inflection point of  $\mathcal{R}_{\text{TE}}$ , is  $68^\circ$ , which agrees with the critical angle defined by Snell's law.

Owing to absorption, the transition to high reflection is not as abrupt as with total internal reflection from trans-

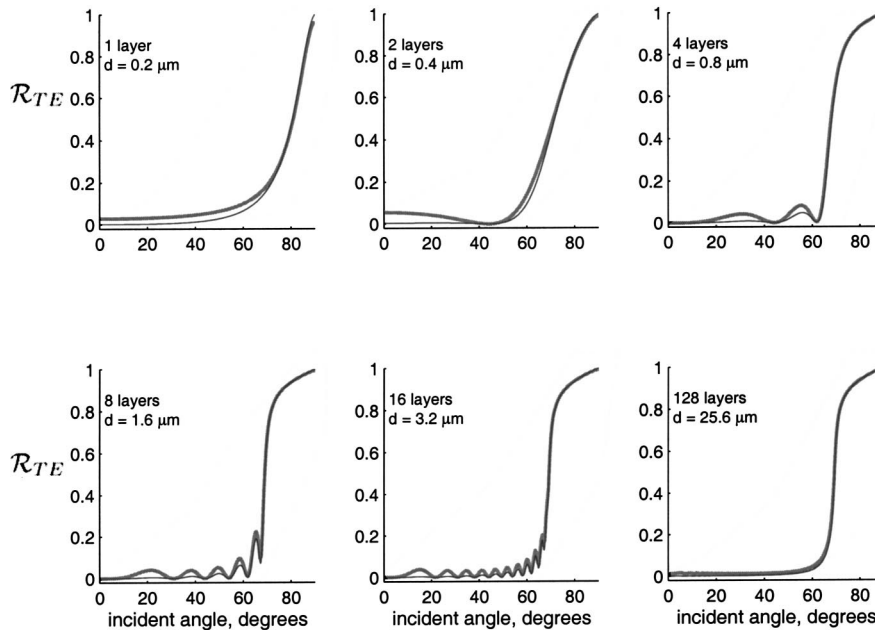


Fig. 7. TER: reflectivity at  $\lambda_0 = 0.5 \mu\text{m}$  as a function of incident angle. Thick curve, TMM predictions for silver wire metamaterials. Thin curve, analytical calculations based on Fresnel formulas for homogeneous  $n = 0.935 + 0.0038i$  slabs of the same thickness as the metamaterial. Wire radius,  $r = 15 \text{ nm}$ ; unit-cell size,  $a = 200 \text{ nm}$ ; homogeneous slab thickness  $d$ .

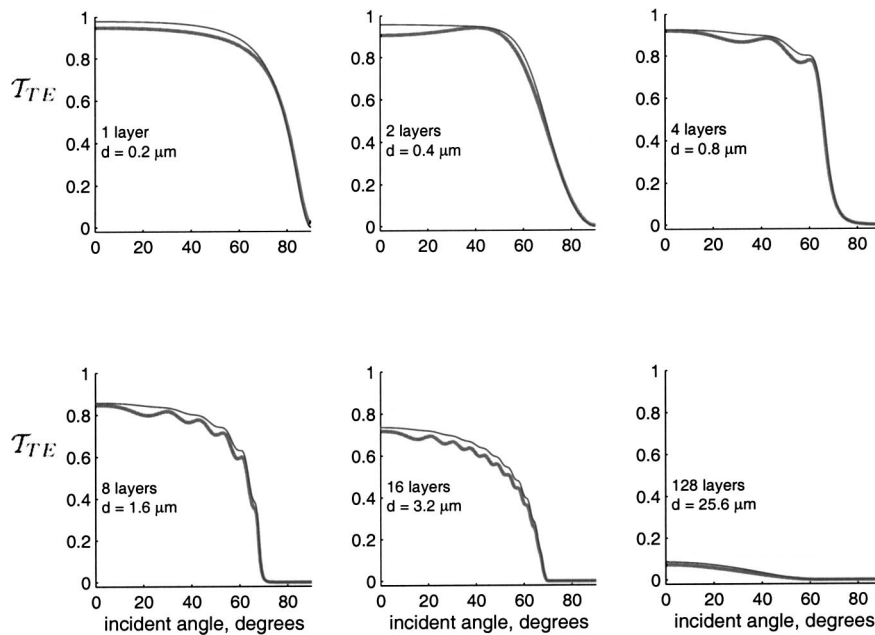


Fig. 8. Transmission at  $\lambda_0 = 0.5 \mu\text{m}$  as a function of incident angle. Thick curve, T-MM predictions for silver wire metamaterials. Thin curve, analytical calculations based on Fresnel formulas for homogeneous  $n = 0.935 + 0.0038i$  slabs of the same thickness as the metamaterial. Wire radius,  $r = 15 \text{ nm}$ ; unit-cell size,  $a = 200 \text{ nm}$ ; homogeneous slab thickness  $d$ .

parent dielectrics, much like the known TER of x rays. Note that, with only four rows of wires, there is a critical angle above which, loss notwithstanding, TER occurs. As a consequence, just a few periods may suffice for practical applications of this effect, easing the fabrication. The effective index properly describes the behavior of the slab even for the case of two layers of wires, a property that could not have been predicted with the long-wavelength approximation. Also note that  $\mathcal{R}_{\text{TE}} + \mathcal{T}_{\text{TE}} < 1$  because of losses.

Hence the reflection data can be used as an alternative method to calculate the refractive index. We calculated the complex refractive index of a homogeneous dielectric slab whose reflectivity best matches that of the finite wire array at all incident angles for polarization normal to the incident plane (TE) and parallel to the wires. That is, we determined the effective index by comparing the reflectivity of the metamaterial with that of a homogeneous material as predicted by the Fresnel formulas. This method also differs from those that use only single-angle incidence reflection and transmission coefficients<sup>8,25</sup> and should give a more reliable value that is appropriate for all incident angles despite the slight anisotropy due to a relative large unit cell. The results are summarized in Fig. 6 and show a striking agreement with the effective index obtained with refraction (Section 5).

## 7. DISCUSSION

The designed ULIM behaves on refraction, reflection, and transmission as a low-loss dielectric with  $0 \leq \text{Re}\{n_{\text{eff}}\} \leq 1$  for wavelengths between roughly  $0.45$  and  $1.2 \mu\text{m}$ , as shown in Fig. 6. The reflectivity at shorter wavelengths ceases to resemble TER because  $\lambda$  approaches  $2a$ . At longer wavelengths, loss dominates as  $\text{Re}(n_{\text{eff}})$  decreases, and the reflectivity resembles that of a high-loss dielec-

tric. Note that even though the metamaterial is lossy and dispersive, for a proper design the attenuation of waves propagating in the metamaterial is much lower than in metals at optical frequencies. Although in metals at optical wavelengths the imaginary part of the refractive index dominates, in the metamaterial it can be more than 2 orders of magnitude smaller than the real part. Note that the use of real parameters for the composing materials (including losses and dispersion) is critical to achieve an accurate picture because optical properties of metals do not scale with frequency.

The zero-permittivity materials ( $\epsilon_{\text{eff}} = 0$ ) recently proposed as bandgap structures<sup>14</sup> can be considered a limiting case of the ULIMs presented here ( $0 \leq \text{Re}\{n_{\text{eff}}\} \leq 1$ ). However, they do not show the effect of TER defined by a critical angle different from zero. Moreover, our calculations indicate that losses produced by real metals should play a critical role at optical frequencies in the  $\epsilon \rightarrow 0$  limit, suggesting that, in this limiting case, further investigation is required.

Note that dielectric photonic bandgap materials can also refract light incident in vacuum away from the surface normal for frequencies close to the bandgap. Thus one could assign them a refractive index less than unity and even less than zero that will be consistent with Snell's law.<sup>24</sup> However, this effect differs from the reflection from ULIM: (a) the photonic bandgap materials do not, in principle, have the same angle-dependent reflectivity and transmissivity predicted by Fresnel formulas, (b) their unusual values of refractive index apply only to narrow bandwidths, and (c) they require a bandgap.

We are currently exploring the space of attainable dielectric constants with two homogeneous materials.<sup>9</sup> Although the presence of a metal is critical, its relative volume to different dielectrics and unit-cell structure can be changed according to design constraints.

In conclusion, we have analyzed optical metamaterials with  $0 \leq \text{Re}\{n_{\text{eff}}\} \leq 1$  at optical frequencies by using approximate analytical models and accurate numerical models. We used real data for the metal to provide an accurate picture of the effect of losses and dispersion. Methods for determining a realistic effective index based on reflected and refracted fields were implemented. To the best of the authors' knowledge, this is the first time a metamaterial has been shown to exhibit total external reflection at optical visible wavelengths. No bandgap is required to observe this effect. Such flexibility in the specification of the effective properties of a material opens up new opportunities for device applications.

## ACKNOWLEDGMENTS

B. T. Schwartz thanks Andrew L. Reynolds for his assistance with Translight transfer-matrix software and acknowledges partial support by the National Science Foundation under grant 9870665 to the University of Colorado through the National Science Foundation Integrative Graduate Education and Research Traineeship Program.

B. T. Schwartz can be reached by e-mail at Brian.Schwartz@colorado.edu.

## REFERENCES

1. J. D. Joannopoulos, R. D. Meade, and J. N. Winn, *Photonic Crystals* (Princeton U. Press, Princeton, N.J., 1995).
2. R. A. Shelby, D. R. Smith, and S. Schultz, "Experimental verification of a negative index of refraction," *Science* **292**, 77–79 (2001).
3. J. B. Pendry, "Negative refraction makes a perfect lens," *Phys. Rev. Lett.* **85**, 3966–3969 (2000).
4. P. M. Valanju, R. M. Walser, and A. P. Valanju, "Wave refraction in negative-index media: always positive and very inhomogeneous," *Phys. Rev. Lett.* **88**, 187401 (2002).
5. N. Garcia and M. Nieto-Vesperinas, "Is there an experimental verification of a negative index of refraction yet?" *Opt. Lett.* **27**, 885–887 (2002).
6. N. Garcia and M. Nieto-Vesperinas, "Left-handed materials do not make a perfect lens," *Phys. Rev. Lett.* **88**, 207403 (2002).
7. B. T. Schwartz and R. Piestun, "Total external reflection at optical wavelengths," in *Diffraction Optics and Micro-Optics*, R. Magnusson, ed., Vol. 75 of OSA Trends in Optics and Photonics (Optical Society of America, Washington D.C., 2002), pp. 175–177.
8. J. Brown, "Artificial dielectrics," *Prog. Dielectr.* **2**, 193–225 (1960).
9. D. E. Aspnes, "Local-field effects and effective medium theory: a microscopic perspective," *Am. J. Phys.* **50**, 704–709 (1982).
10. D. Felbacq and G. Bouchitté, "Homogenization of a set of parallel fibres," *Waves Random Media* **7**, 245–256 (1997).
11. J. Brown, "Artificial dielectrics having refractive indices less than unity," *Proc. IEE* **100C**, 51–62 (1953).
12. K. C. Gupta, "Narrow-beam antennas using an artificial dielectric medium with permittivity less than unity," *Electron. Lett.* **7**, 16–17 (1971).
13. S. Enoch, G. Tayeb, P. Sabouroux, N. Guerin, and P. Vincent, "A metamaterial for directive emission," *Phys. Rev. Lett.* **89**, 213902 (2002).
14. N. Garcia, E. V. Ponizovskaya, and J. Q. Xiao, "Zero permittivity materials: band gaps at the visible," *Appl. Phys. Lett.* **80**, 1120–1122 (2002).
15. D. Sievenpiper, "High-impedance electromagnetic surfaces," Ph.D. thesis (University of California at Los Angeles, Los Angeles, Calif., 1999).
16. D. Attwood, *Soft X-Rays and Extreme Ultraviolet Radiation: Principles and Applications* (Cambridge U. Press, Cambridge, U.K., 1999).
17. J. B. Pendry, A. J. Holden, D. J. Robbins, and W. J. Stewart, "Low frequency plasmons in thin-wire structures," *J. Phys.: Condens. Matter* **10**, 4785–4809 (1998).
18. J. R. Reitz, F. J. Milford, and R. W. Christy, *Foundations of Electromagnetic Theory*, 4th ed. (Addison-Wesley, Reading, Mass., 1993).
19. D. W. Lynch and W. R. Hunter, "Comments on the optical constants of metals and an introduction to the data for several metals," in *Handbook of Optical Constants of Solids*, E. D. Palik, ed. (Academic, San Diego, Calif., 1991), pp. 275–368.
20. A. L. Pokrovsky and A. L. Efros, "Electrodynamics of metallic photonic crystals and the problem of left-handed materials," *Phys. Rev. Lett.* **89**, 093901 (2002).
21. R. M. Walser, A. P. Valanju, and P. M. Valanju, "Comment on 'Extremely low frequency plasmons in metallic mesostructures'," *Phys. Rev. Lett.* **87**, 119701 (2001).
22. W. Rotman, "Plasma simulation by artificial dielectrics and parallel-plate media," *IRE Trans. Antennas Propag.* **AP10**, 82–95 (1962).
23. *Ansoft HFSS Version 8.0.25* (Ansoft Corporation, Pittsburgh, Pa., 2001).
24. M. Notomi, "Theory of light propagation in strongly modulated photonic crystals: refraction-like behavior in the vicinity of the photonic bandgap," *Phys. Rev. B* **62**, 10696 (2000).
25. D. R. Smith, S. Schultz, P. Markos, and C. M. Soukoulis, "Determination of effective permittivity and permeability of metamaterials from reflection and transmission coefficients," *Phys. Rev. B* **65**, 195104 (2002).
26. O. Acher, A. L. Adenot, and F. Duverger, "Fresnel coefficients at an interface with a lamellar composite material," *Phys. Rev. B* **62**, 13748–13756 (2000).
27. *Femlab Version 2.30.145* (Comsol Corporation, Burlington, Mass., 2002).
28. G. Guida, D. Maystre, G. Tayeb, and P. Vincent, "Mean-field theory of two-dimensional metallic photonic crystals," *J. Opt. Soc. Am. B* **15**, 2308–2315 (1998).
29. P. M. Bell, J. B. Pendry, L. M. Moreno, and A. J. Ward, "A program for calculating photonic band structures and transmission coefficients of complex structures," *Comput. Phys. Commun.* **85**, 306–322 (1995).
30. A. L. Reynolds, *Translight Software* (Optoelectronics Research Group, Dept. of Electronics and Electrical Engineering, Univ. of Glasgow, Glasgow, Scotland, 2000).